

The November 10, 2002 Tennessee Tornadoes: A Spring WES Drill for Forecasters at WFO Salt Lake City, Utah

Mark Jackson , WFO Salt Lake City, UT
July 1, 2003

Introduction

The Veteran's Day weekend tornado outbreak of November 9-11, 2002 was the second largest November tornado outbreak on record over the eastern United States. Over this period seventy-six tornadoes were reported in seventeen states, resulting in 36 fatalities (National Weather Service 2003). One of the more active areas for severe weather in this period was in the Nashville, Tennessee, WFO County Warning Area (CWA, [Fig. 1](#)), where two distinct severe weather episodes occurred over less than a 24-h period. The first episode occurred during the night of 9 November and continued into the early morning hours of 10 November. Four tornadoes were reported during this first period in the Nashville WFO CWA. The second episode, and the focus of this paper, was part of a larger severe weather outbreak across an area from Mississippi northeast into Ohio and Pennsylvania. This paper will focus on a family of tornadic supercells that formed ahead of the surface cold front and moved northeast across the southeastern third of the WFO Nashville's CWA during the late afternoon and early evening of 10 November. [Figure 2](#) depicts severe wind and hail reports reported in the Nashville WFO CWA between 2100 UTC, 10 November, and 0259 UTC, 11 November, while [Fig. 3](#) depicts tornado reports within this same area during this time. These supercells exhibited classic tornadic structure as depicted by the Nashville WSR-88D (KOHX), forming in a strongly sheared and moderately unstable environment. The environmental conditions that spawned these storms emphasizes the importance of analyzing and understanding these volatile conditions prior to onset of the event, further assisting the warning decision making process through heightened situational awareness. This paper will also briefly discuss severe weather occurrences associated with the strong cold front that entered the area from the northwest.

Drill Design

This case was recently used as a spring drill for forecasters at WFO Salt Lake City, Utah, using the AWIPS Weather Event Simulator (WES) localized for WFO Nashville. Though events of this magnitude are unlikely to occur in Utah, understanding and reviewing tornadic environments and supercell structure through a case such as this strengthens the foundation of knowledge necessary when placed in any severe weather situation - even in Utah. Most importantly, the drill simulates and provides practice for an active operational warning environment to be applied to actual warning situations of any degree of magnitude.

The drill begins at 1800 UTC, Sunday, 10 November. This initial step instructed and tested the knowledge and understanding of determining the ingredients necessary for severe weather based on evaluating the current and forecast environment, including understanding the predominant type, location, and timing of potential severe weather. Next, the D2D clock was moved forward to 2300 UTC, a time when supercell development had already begun across the WFO Nashville CWA. Forecasters worked in pairs to simulate an operational warning team environment. One forecaster was in charge of operating D2D, including using WarnGen to define and issue warnings, while the second forecaster - also part of the warning decision making process - was in charge of tracking warning issuance and valid times, location, and verification. Verification was received from the drill monitor (e.g. the SOO) reading reports in simulated real time and extracted from a combination of the Nashville WFO Local Storm Report filed for this case, and times corrected from the NWS Service Assessment. The warning team was in charge of issuing warnings in this CWA through 0100 UTC 11 November.

Environmental Conditions

This tornado outbreak was a result of multiple classic factors. Moller et al (1994) provide a comprehensive look at recognizing supercell environments and storm structures in forecast operations. They suggest forecasters use a two-stage procedure in determining supercell potential. The first is determining the temporal and spatial limits of deep, moist convection through accurate diagnosis of moisture, instability, and mesoscale lifting mechanisms. Secondly, the forecaster should determine where and when within the convective forecast area the combination of vertical windshear and CAPE is conducive for mesocyclones. Diagnosing the possible existence of these and other conditions conducive to severe weather was the first step for forecasters completing during this WES drill, understanding that heightened situational awareness prior to an event can significantly and positively contribute to the warning decision making process.

Figures [4](#), [5](#), and [6](#) present the upper air analyses at 300-, 500- and 850-mb respectively at 1200 UTC on 10 November. A deep upper trough moved through the eastern half of the United States during 9-11 November. This trough was comprised of multiple shortwaves, the first of which moved through western and central Tennessee during the night of 9-10 November and shown in the Eta 500-mb analysis (see [Fig. 5](#)). Storms associated with this system produced 10 tornadoes and resulted in 4 fatalities within the Nashville WFO CWA. A second and deeper short wave, this associated with a strong surface cold front, moved through the Mississippi and Ohio River Valleys, continuing eastward during the afternoon of 10 November and early morning hours of 11 November. Associated with this trough was a strong upper level jet (see [Fig. 4](#)), whose exit region was forecast to be approximately over the middle Mississippi Valley at 0000 UTC 11 November, or late Sunday afternoon 10 November CST. Coincident with this upper level jet was an increasingly strong jet core at low levels. The 850-Mb analysis (see [Fig. 6](#)) shows this jet at low levels, in addition to abundant low-level moisture. To further diagnose the jet structure affecting the warning area, [Fig. 7](#) is a 3-dimensional look at this jet as analyzed by ETA model initialized at 1200 UTC on 10 November, and displayed using the NOAA/Forecast Systems Laboratory's Display 3-Dimension (D3D, McCaslin et al 2000). The slice in this figure depicts the jet building downward over the 12-h period beginning at 1200 UTC. The increasing low level winds up to 1800 UTC can be verified upon examination of the Okolona, MS profiler

time-height ([Fig. 8](#)). It's possible that the downward propagation of this jet was a result of intensification of an increased isallobaric wind component as the upper jet exit region approached the area (Uccellini and Johnson 1979).

A special sounding was collected at 1800 UTC ([Fig. 9](#)) at the Nashville WFO. The sounding shows a moderately unstable airmass in place at midday with a CAPE of 1549 J/KG; considered sufficient for tornadic supercells based on the work of Rasmussen and Blanchard (1998), who derived a baseline climatology of sounding-derived supercell and tornado forecast parameters. Of even higher significance is the low-level shear profile already in place over the area at 1800 UTC, and as previously discussed, forecast to increase through the day. The Storm Relative Helicity (SRH) based on the 1800 UTC OHX sounding was $456 \text{ m}^2/\text{s}^2$. Again, referencing the results of Rasmussen and Blanchard, this falls well within the determined values conducive to tornadic supercells (NOTE: While helicity calculations are relatively easy to derive and use, forecasters must use helicity with caution in operational situations understanding it is subject to rapid temporal and spatial changes.(See Markowski et al 1998). Finally, as a measure of the combined effect of shear and buoyancy, the Bulk Richardson Number (BRN, Weisman and Klemp 1982, 1984) is often used as a discriminator between ordinary (multi-cellular) convection and supercells. BRN values between 10 and 40 favor supercells, while values less than this range define weak shears unable to sustain organized convection. [Figure 10](#) is the 3-h MesoEta forecast (valid 2100 UTC 10 November) of BRN and CAPE, and overlaid with the MesoEta boundary layer wind. BRN values were forecast to be above 15 during this time period, within the acceptable range for supercell development, and potentially tornadic.

The one caveat to supercell development in this case is the fairly unidirectional component of the lower- and upper-level jets. Barnes and Newton (1986) derived an idealized sketch of a mid-latitude synoptic-scale situation favorable for development of severe thunderstorms, including supercell-induced tornadoes. The vertical jet structure in this conceptual model exhibits some degree of directional shear between the lower- and upper-level jets Meanwhile, a jet structure conducive to squall line development has been found in case studies (e.g. Duke and Rogash 1992) to have a low-level jet more parallel to the upper-level jet - as was more the case with this event (even though there was moderate directional shear in the 0-3 km AGL layer). This particular case was characterized by supercell development ahead of a strong squall-line primarily associated with the intense lift along the strong cold front. This presented two distinct warning scenario challenges for forecasters completing the drill - one of identifying and warning for supercells and their associated severe weather, and a second near and along the squall-line which produced strong, damaging outflow winds.

In addition to the synoptic-scale forcing during this event, another important mesoscale feature deserves mention. Though not readily apparent in the surface observations, a possible low-level boundary is evident on the 1800 UTC GOES-8 visible image ([Fig. 11](#)). The two arrows in this figure point out evidence of two surface convergence boundaries, possibly a result of convection in the area the night before. These boundaries may have played a significant role in the development of a family of tornadic supercells that formed ahead of the squall-line and cold front to the west. In their study to determine the influence of preexisting boundaries on supercell evolution, Atkins et al (1999) - using a three-dimensional nonhydrostatic cloud model - found that when boundaries are present the low-level mesocyclone forms much earlier, is stronger, and more persistent than if no boundary is present. Understanding this, and knowing that these boundaries are not always detectable with standard surface observation spacing, emphasizes the use of visible satellite imagery in analyzing the severe convective potential.

Based on these factors, it can be concluded that conditions were favorable for possible long-lived, tornadic supercells, along with strong convection associated with a developing squall-line ahead of and along the surface cold front. The NWS Storm Prediction Center's day one convective outlook issued that morning placed the area within a "High Risk" of severe weather ([Fig. 12](#)).

Development and Lifecycle of the Tornadic Supercells and Squall-line

At 2115 UTC ([Fig. 13](#)), the two main areas of convection were along a line associated with the main cold front, which at this time was situated northwest of the Nashville CWA, and isolated ahead of this line along a southwest-northeast axis dissecting the Nashville CWA. This second area would be the focus of family of intense tornadic supercells over the next 4-6 hours. The initial southward advancement of the activity associated with the cold front, and the development of the tornadic supercells, is best seen in a [loop](#) of 0.5° elevation KOHX WSR-88D reflectivity, covering the period from 2115 - 2357 UTC. Note by 2322 UTC ([Fig. 14](#)) there are four distinct supercells dotted southwest to northeast just to the south of Nashville, denoted A-D, and one just exiting the WFO Nashville CWA . The unlabeled supercell in the northeast corner of the CWA in [Fig. 14](#) produced what was later determined to be an F2 tornado in Fentress County, TN. These intense supercells moved mainly along a southwest-northeast direction, varying little from the mean steering flow, and at speeds of between 40 and 50 mph - as a result passing over the same areas at 30- to 90-minute intervals. Only slight motions to the right of the flow were observed with little if any storm splitting and little change in the orientation of the line. The excessive storm speed further complicated the warning decision process (i.e. avoiding overlapping warnings).

Though each of these supercells produced a tornado at one time during their lifecycles, it's important to try to understand when supercell signatures, such as strong mid-level rotation (mesocyclone), result in tornado occurrences, and when they do not. Recent severe storm field studies (e.g. VORTEX, Rasmussen et al 1994) have revealed, among other things, that strong tornadoes may in fact occur *without* the presence of a strong mid-level mesocyclone and the downward development of rotation, or at a location away from the mesocyclone (Wakimoto and Atkins 1996). On the other hand, there were times that these supercells showed deep and intense rotation with classic supercell structure, while not producing any tornadoes. The following section takes a closer look at this aspect of the case.

[Figure 15](#) and [Fig. 16](#) are 4-panel displays of the 0.5°, 1.5°, 2.4°, and 3.4° elevation reflectivity (dBZ) and SRM (kt) at 2328 UTC. Cells "A"and "B" both exhibit the classic low-level hook appendage as seen in the 0.5° elevation scan. More impressive are the strong mesocyclones, and the solid Bounded Weak Echo Regions (BWER) visible in the 1.5° elevation scan, and an indication of increasing water and ice content around the updraft core and apparent intensification of the updraft (Lemon and Doswell 1979). The WSR-88D Tornado Vortex Signature (TVS) algorithm detected TVS's in each of these cells. TVS's detected in conjunction with a storm that already has a strong mesocyclone signature should be given special consideration for a tornado warning with that storm (NWS/WDTB 2002). Even greater consideration should given when the storm has recognizable three-dimensional, supercell structure (BWER, developing hook echo, etc). At 2335 UTC supercell "A" produced a weak F0 tornado near Manchester in Coffee County. This same

cell produced tornadoes much later at approximately 0102 UTC over Cumberland County in the extreme northeast portion of the CWA, and at 0102 UTC in Morgan County (just east of the OHX CWA).

It's also during this portion of the drill that the squall-line associated with the surface cold front was moving into the northwest section of the CWA. To demonstrate the use of WSR-88D velocity (not SRM) data, [Fig. 17](#) is a 4-panel display of KOHX WSR-88D 0.5° elevation reflectivity (top left), velocity (lower left), and SRM (lower right). Note the difference between the velocity returns and the SRM with respect to the approaching squall-line. Though SRM more accurately depicts the cell rotation in the supercells to the south of the radar, it misses the strong winds (just off the surface) associated with the line of storms in the northwest, emphasizing the need to use both SRM and velocity in this situation.

Proceeding further into the event, [Figure 18](#) and [Fig. 19](#) show 4-panel displays of the 0.5°, 1.5°, 2.4°, and 3.4° elevation reflectivity (dBZ) and SRM (kt) at 0044 UTC 11 November. At this time the cell (labeled cell "C" in [Fig. 14](#)) over eastern Bedford county is producing an F2 tornado near the Normandy community, and not far from where a previous tornado occurred at 2335 UTC. This cell continued to move rapidly to the northeast, producing another F2 tornado at approximately 0102 UTC in Coffee County and causing significant damage to homes between Fredonia and New Union. [Figure 20](#) is a 4-panel display of 0.5° and 1.5° reflectivity and SRM at 0102 UTC. Once again this cell exhibits classic supercell structure, including a low-level hook appendage, BWER, and deep rotation. Keep in mind that cell "A" is also producing a tornado in Cumberland County around this same time.

These supercells continued to move rapidly to the northeast as the evening progressed. The most damaging tornado of the event over the Nashville WFO CWA occurred at approximately 0343 UTC when an F3 tornado moved through Cumberland County, TN. This tornado had a path length of 12.2 mi, was 400 yards wide, and resulted in 4 fatalities.

Summary

This event presented significant warning decision making challenges, both in real-time at the NWS Nashville WFO, and when administered as a displaced-real-time WES drill to forecasters at the NWS Salt Lake City WFO. It emphasized the importance of understanding the pre-storm environment, recognizing supercell characteristics and associated severe weather, and the characteristics of squall-line development, propagation, and potential as a severe wind producer. Though events of this magnitude are considered an extreme rarity in Utah, the fundamental components that made up the event, along with the operational severe warning procedures that must be efficiently carried out even in a post-event exercise, provide a training experience unmatched through any other training delivery and platform available to NWS forecasters.

References

- Atkins, Nolan T., Weisman, Morris L., Wicker, Louis J. 1999: The influence of preexisting boundaries on supercell evolution. *Mon. Wea. Rev.*, **127**, No. 12, 2910–2927.
- Barnes, S. L., and C.W. Newton, 1986: Thunderstorms in the synoptic setting. *Thunderstorm Morphology and Dynamics*. 2nd ed., E. Kessler, Ed., 75-112.
- Duke, James W., Rogash, Joseph A. 1992: Multiscale review of the development and early evolution of the 9 April 1991 derecho. *Wea. Forecasting*, **7**, No. 4, 623–635.
- Lemon, L. R., and C. A. Doswell III, 1979: Severe thunderstorm evolution and mesocyclone structure as related to tornadogenesis. *Mon. Wea. Rev.*, **107**, No. 9, 1184–1197.
- Markowski, Paul M., Straka, Jerry M., Rasmussen, Erik N., Blanchard, David O. 1998: Variability of storm-relative helicity during VORTEX. *Mon. Wea. Rev.*, **126**, No. 11, 2959–2971.
- McCaslin, P.T., P. A. McDonald, and E. J. Szoke, 2000: [3D Visualization Development at NOAA Forecast Systems Laboratory](#). AMC SIGGRAPH Computer Graphics, February 2000, **34**, No. 1, 41-44.
- Moller, Alan R., Doswell, Charles A., Foster, Michael P., Woodall, Gary R. 1994: The operational recognition of supercell thunderstorm environments and storm structures. *Wea. Forecasting*, **9**, No. 3, 327–347.
- National Weather Service. 2003: Veterans Day Weekend Tornado Outbreak of November 9-11, 2002. Service Assesment. 37 pp.
- National Weather Service/Warning Decision Training Branch. 2002: Tornado Warning Guidance Document 2002. Available on the web at <http://wdtb.noaa.gov/resources/PAPERS/twg02/TWG2002.pdf>.
- Rasmussen, Erik N., Davies-Jones, Robert, Doswell, Charles A., Carr, Frederick H., Elts, Michael D., MacGorman, Donald R., Straka, Jerry M., Carr, Frederick H. 1994: Verification of the Origins of Rotation in Tornadoes Experiment: VORTEX. *Bull. Amer. Meteor. Soc.*, **75**, No. 6, 995–1006.
- _____, Blanchard, David O. 1998: A baseline climatology of sounding-derived supercell and tornado forecast parameters. *Wea. Forecasting*, **13**, No. 4, 1148–1164.
- Uccellini, Louis W., Johnson, Donald R. 1979: The coupling of upper and lower tropospheric jet streaks and implications for the development of severe convective storms. *Mon. Wea. Rev.*, **107**, No. 6, 682–703.
- Wakimoto, Roger M., N. T. Atkins. 1996: Observations and origins of rotation: The Newcastle tornado during VORTEX 94. *Mon. Wea. Rev.*, **124**, No. 3, 384-407.

Weisman, Morris L., Klemp, J.B.. 1982: The dependence of numerically simulated convective storms on vertical wind shear and buoyancy. *Mon. Wea. Rev.*, **110**, No. 6, 504–520.

1984: The structure and classification of numerically simulated convective storms in directionally varying wind shears. *Mon. Wea. Rev.*, **112**, No. 12, 2479–2498.

Figure 1

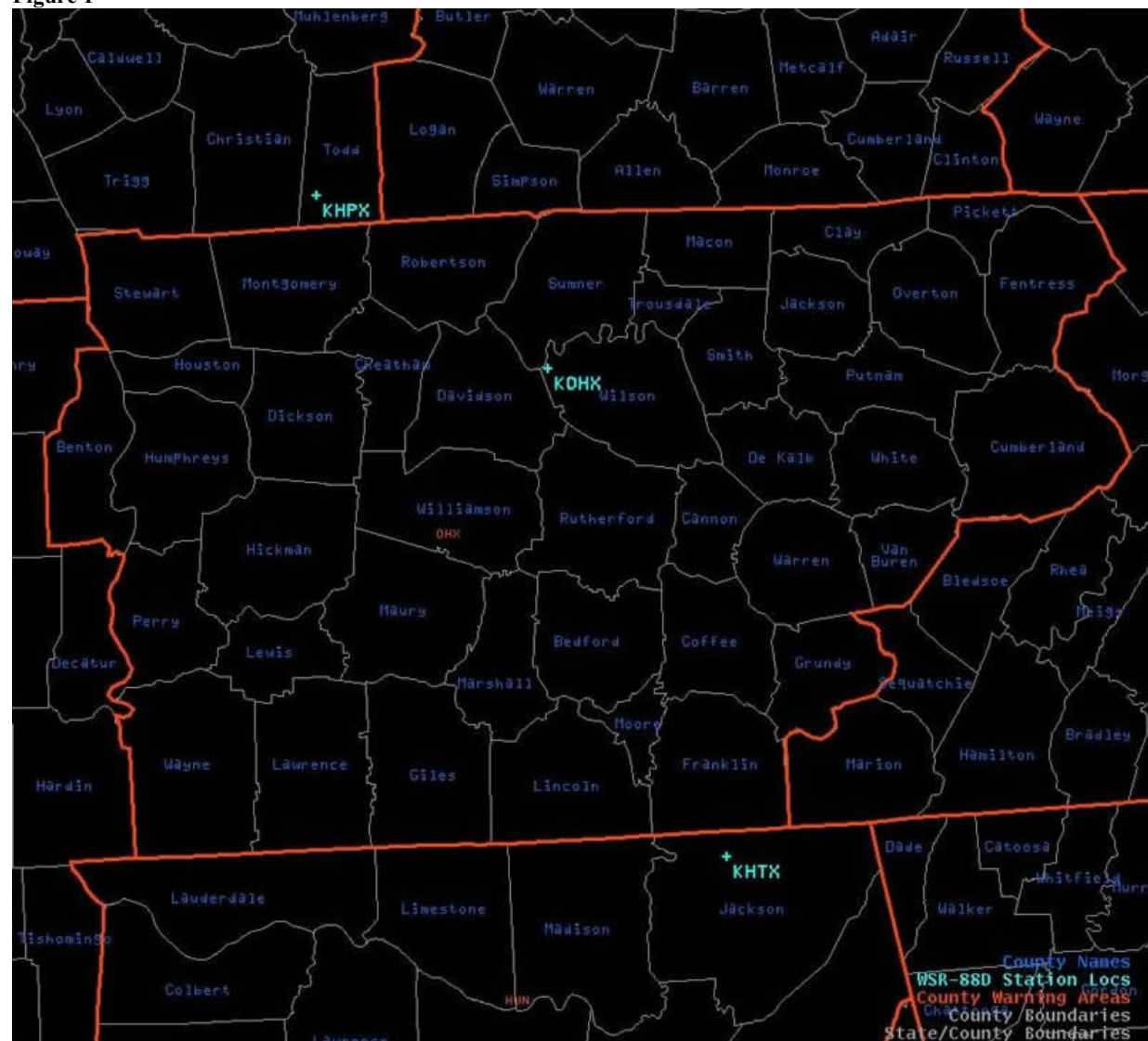


Figure 2

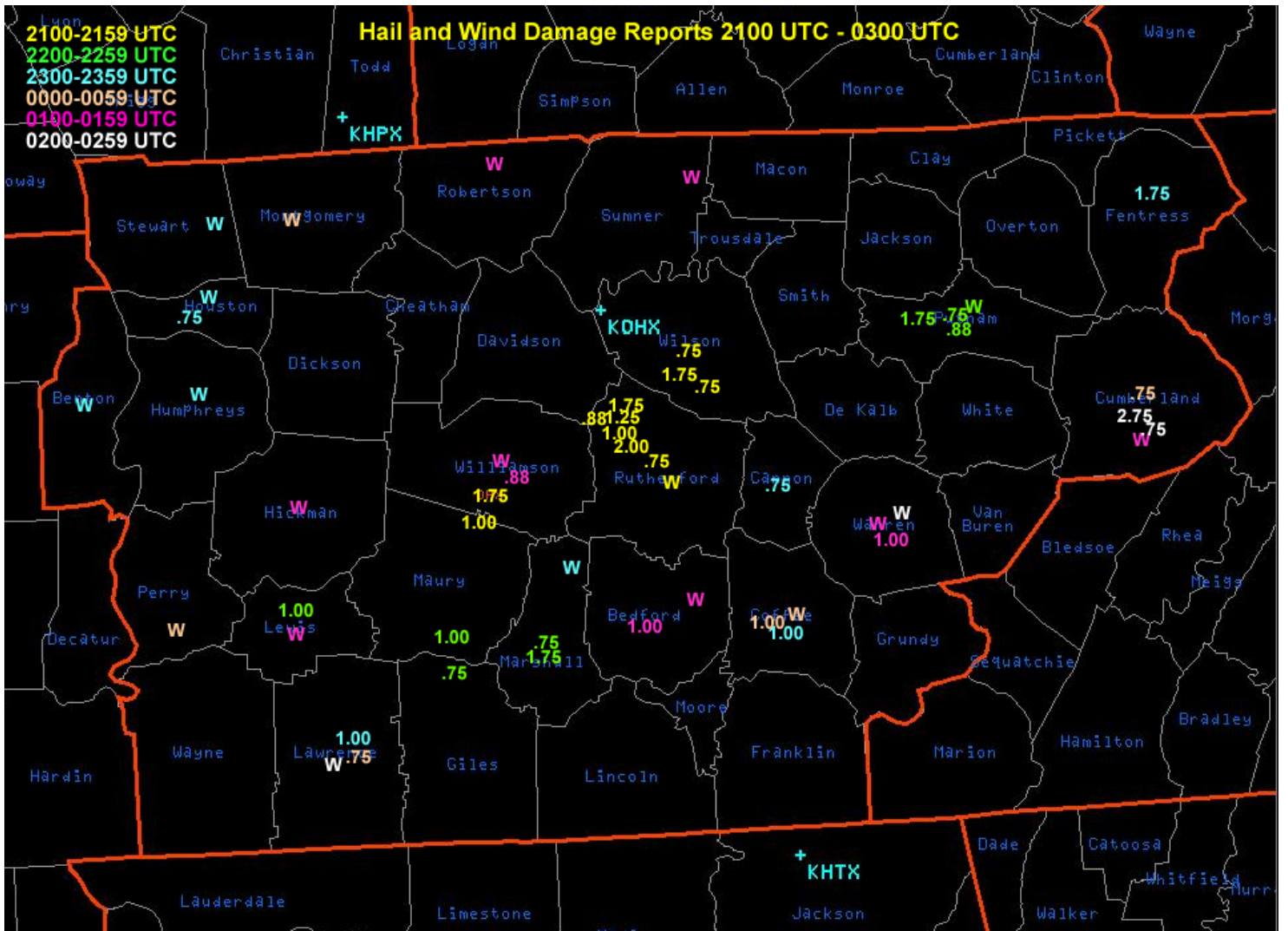


Figure 3

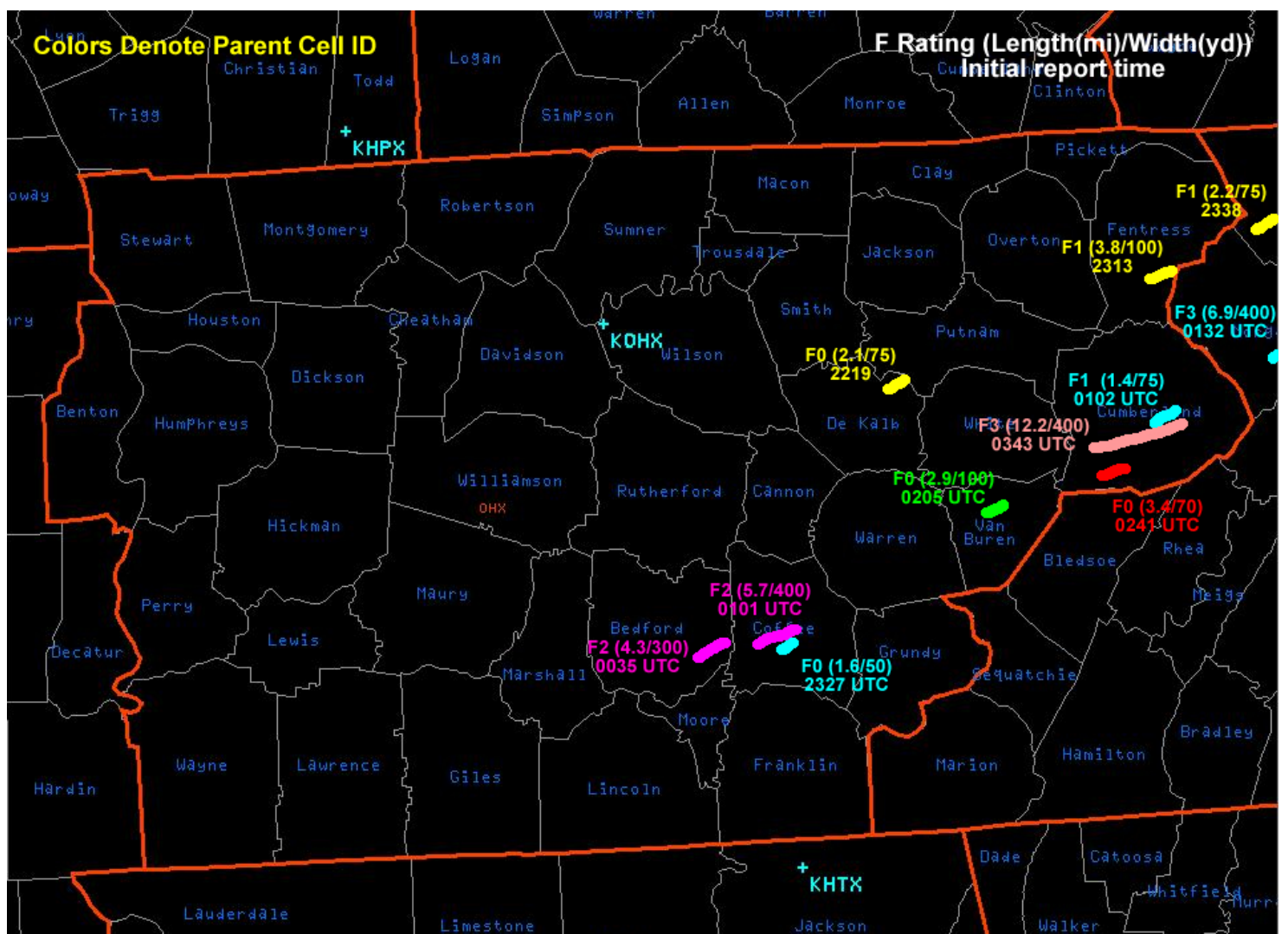


Figure 4

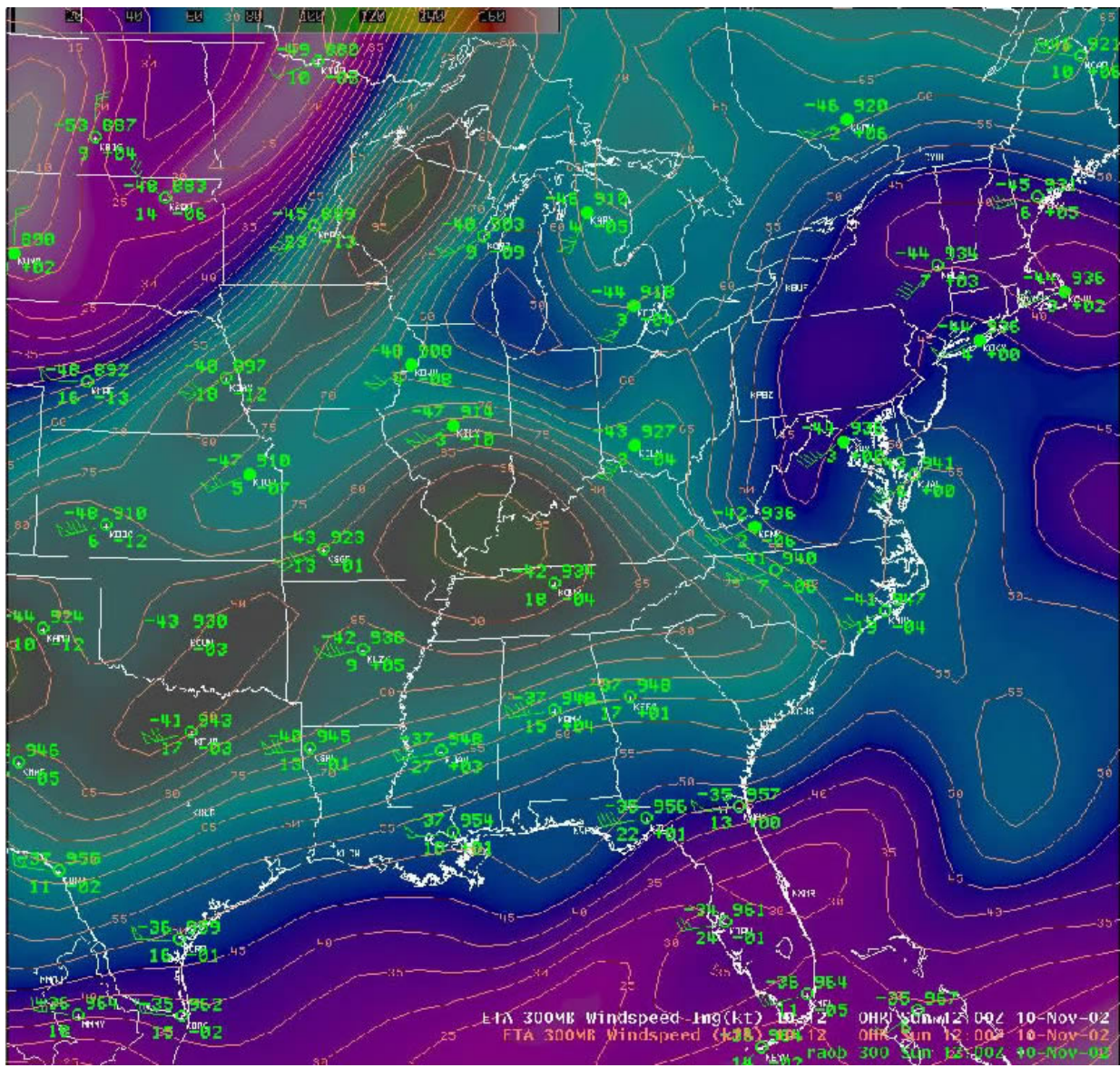


Figure 5

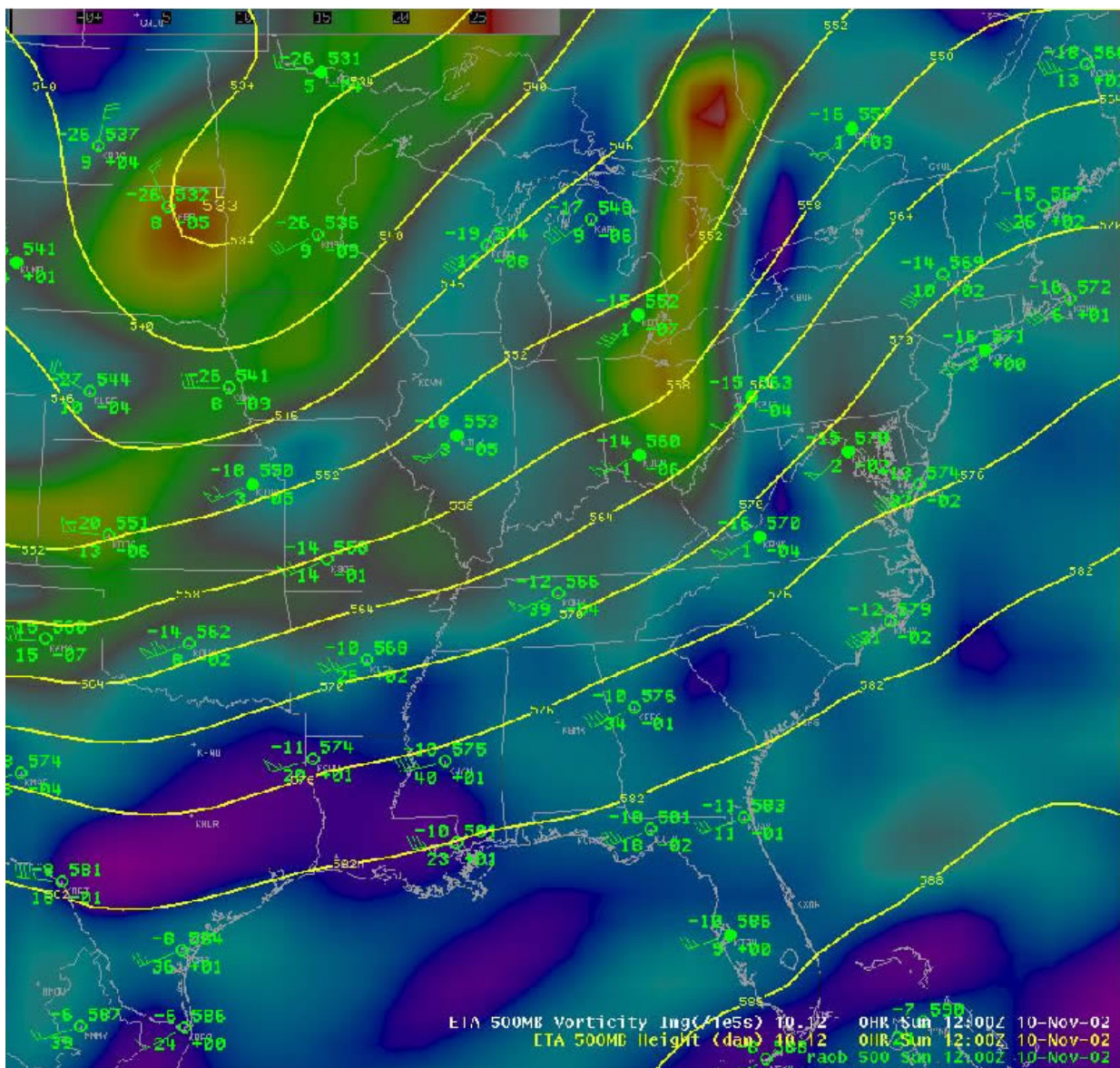


Figure 6

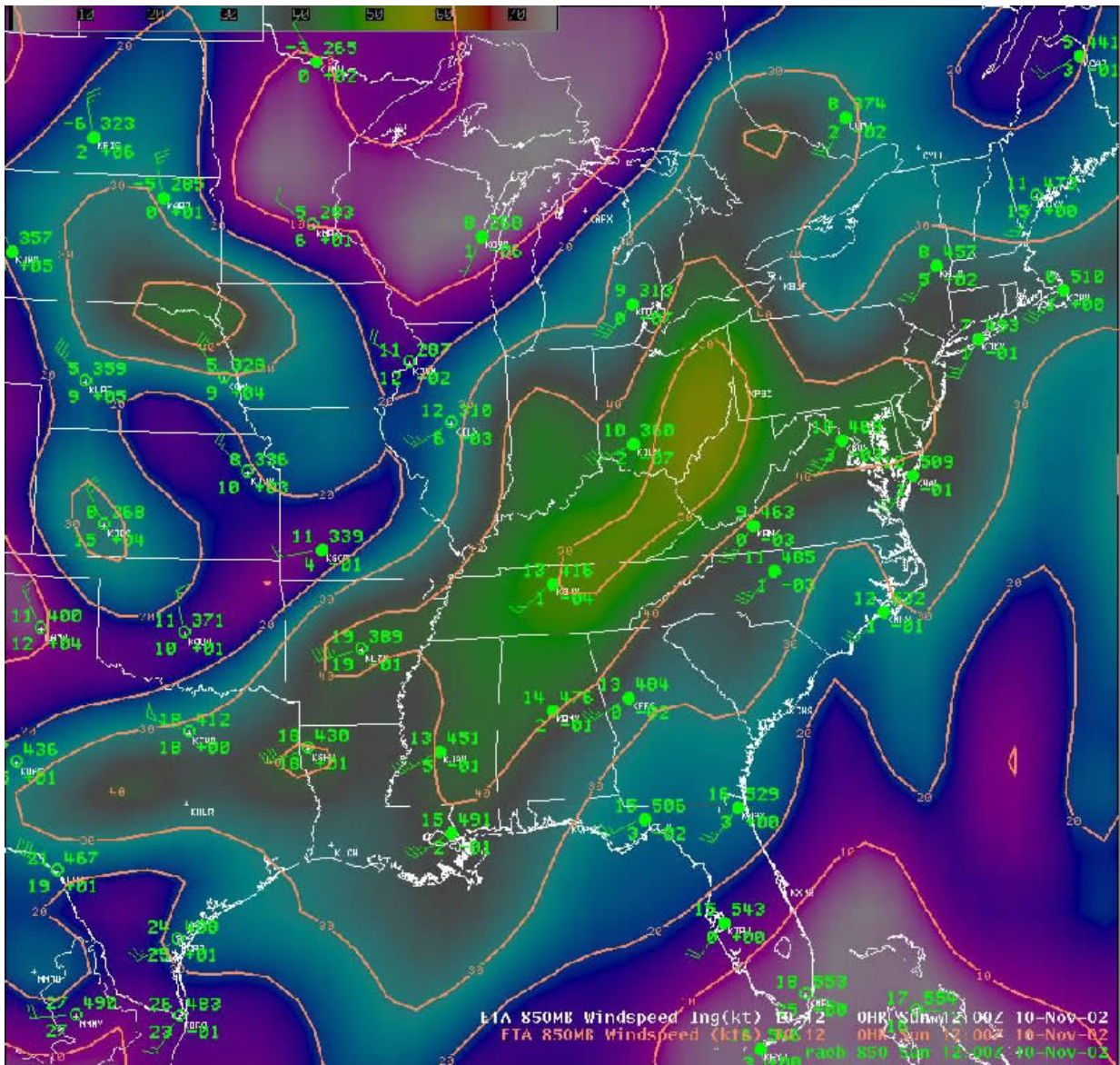


Figure 7

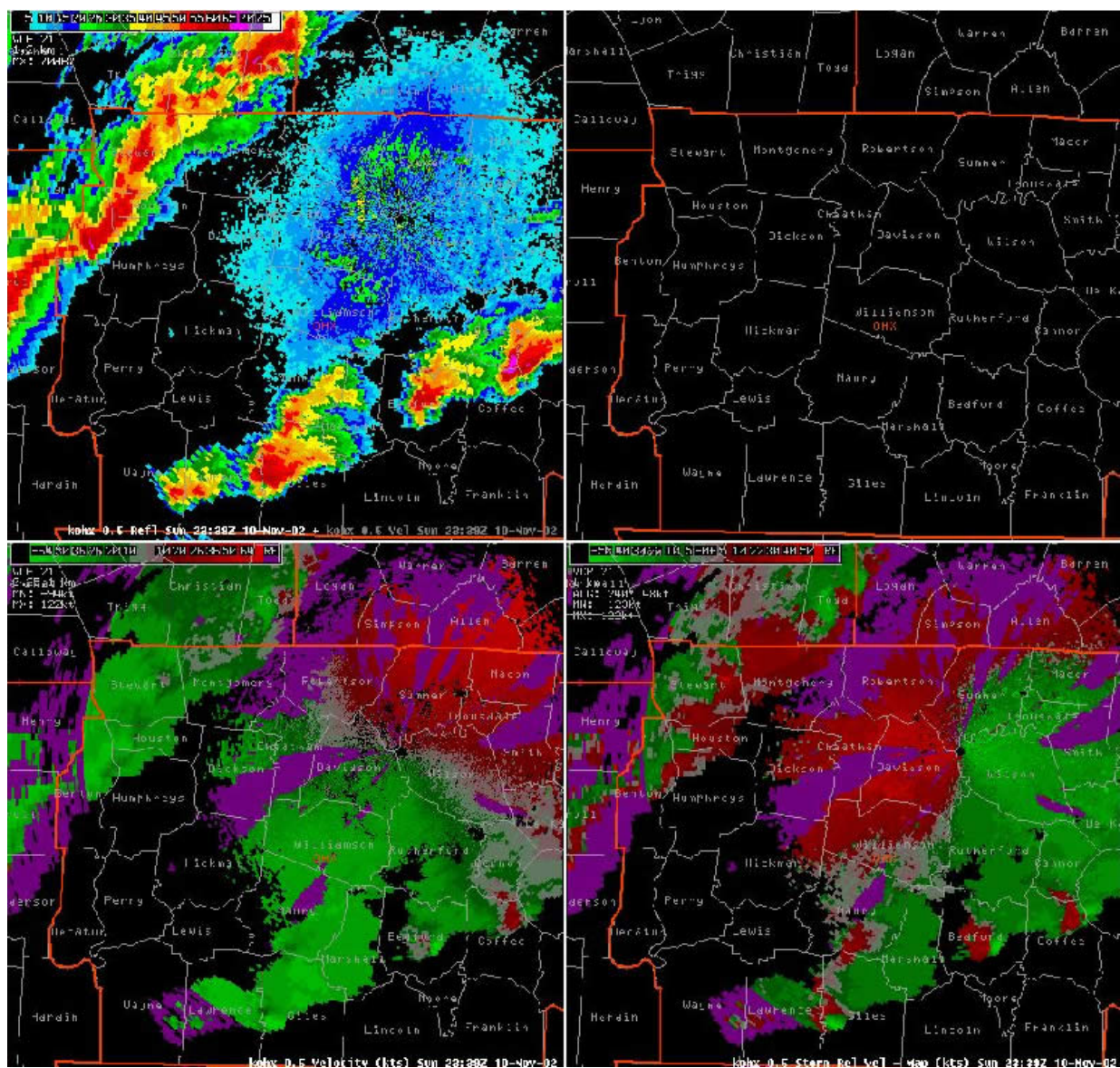


Figure 8

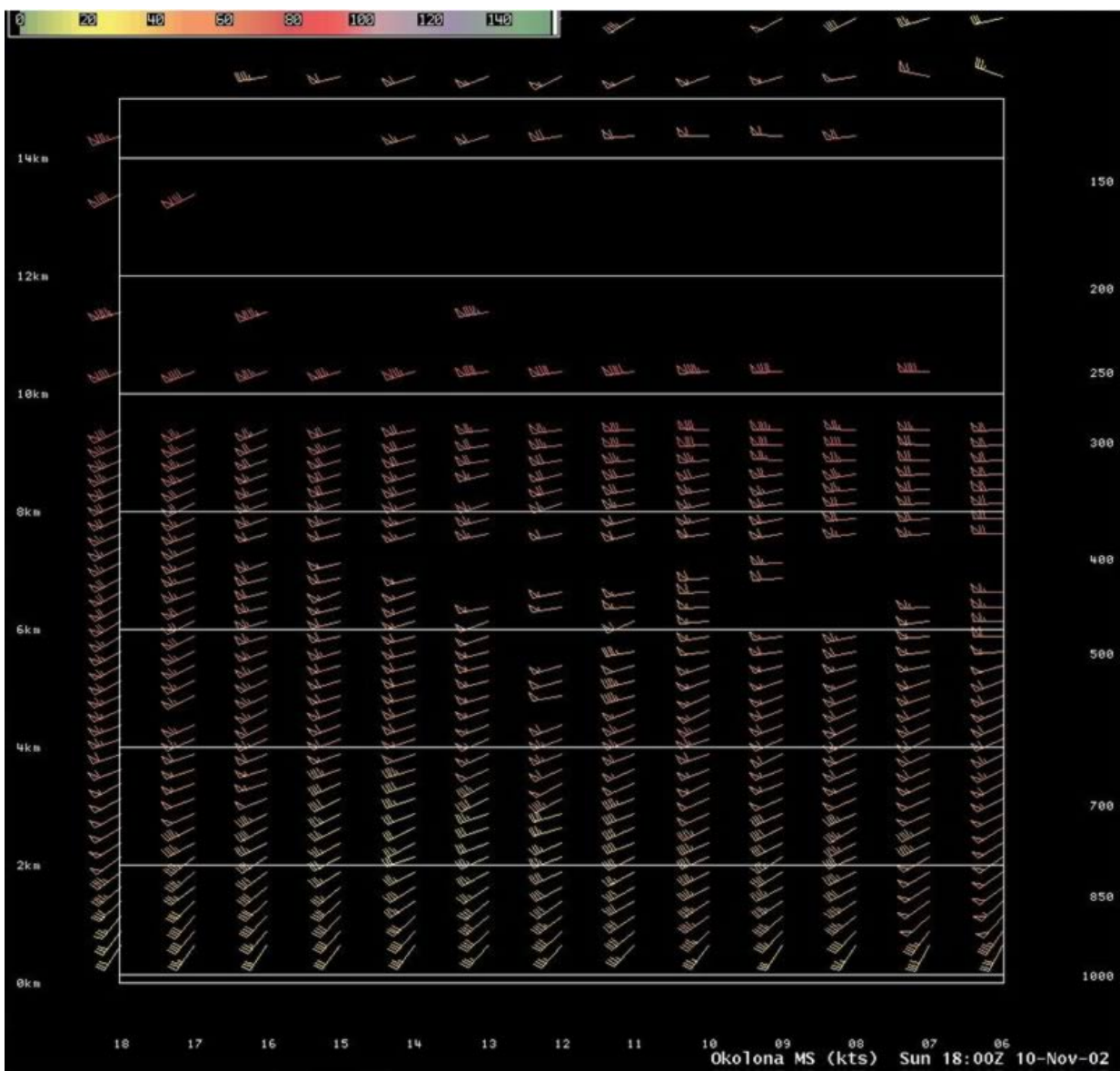


Figure 9

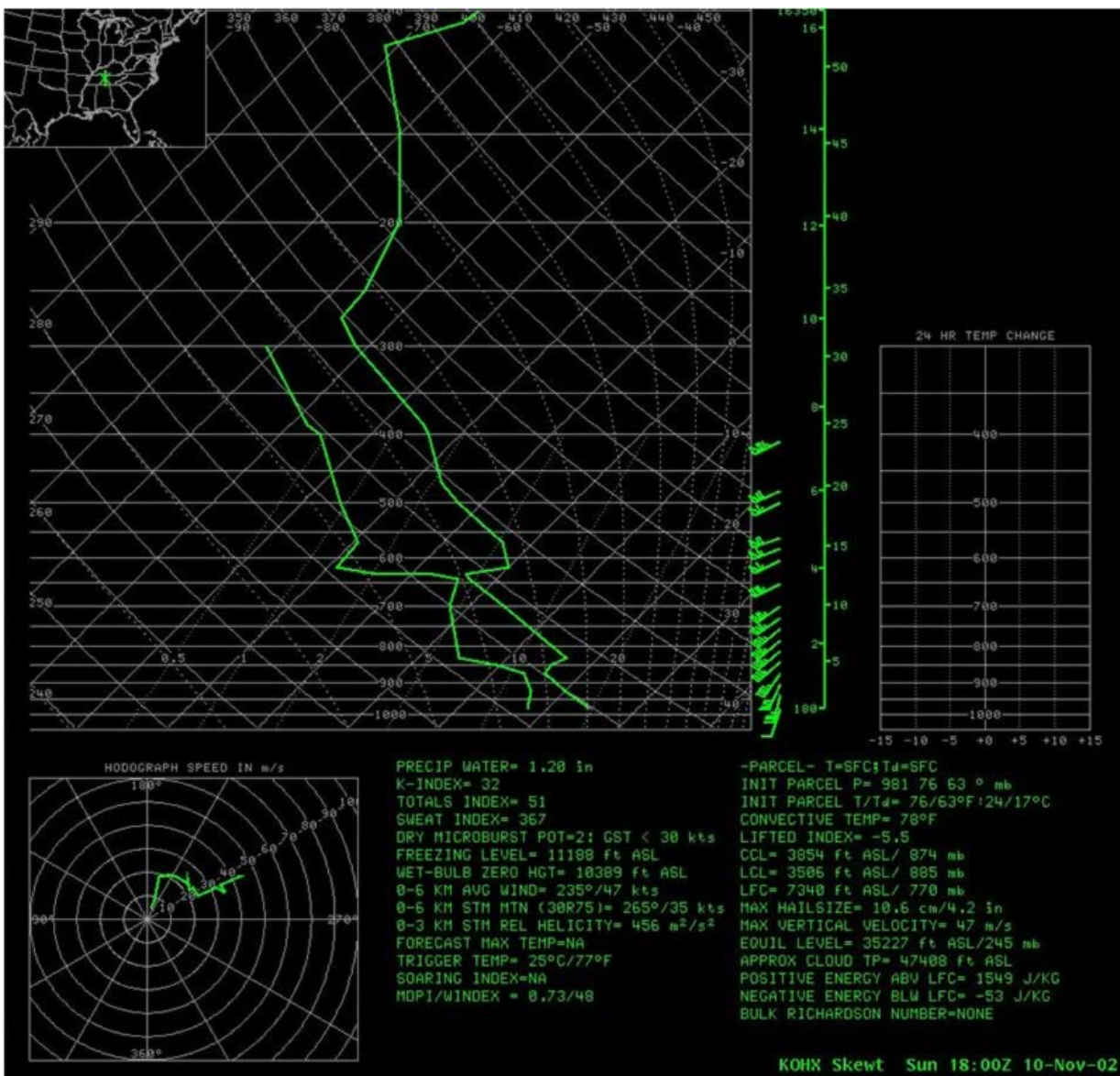


Figure 10

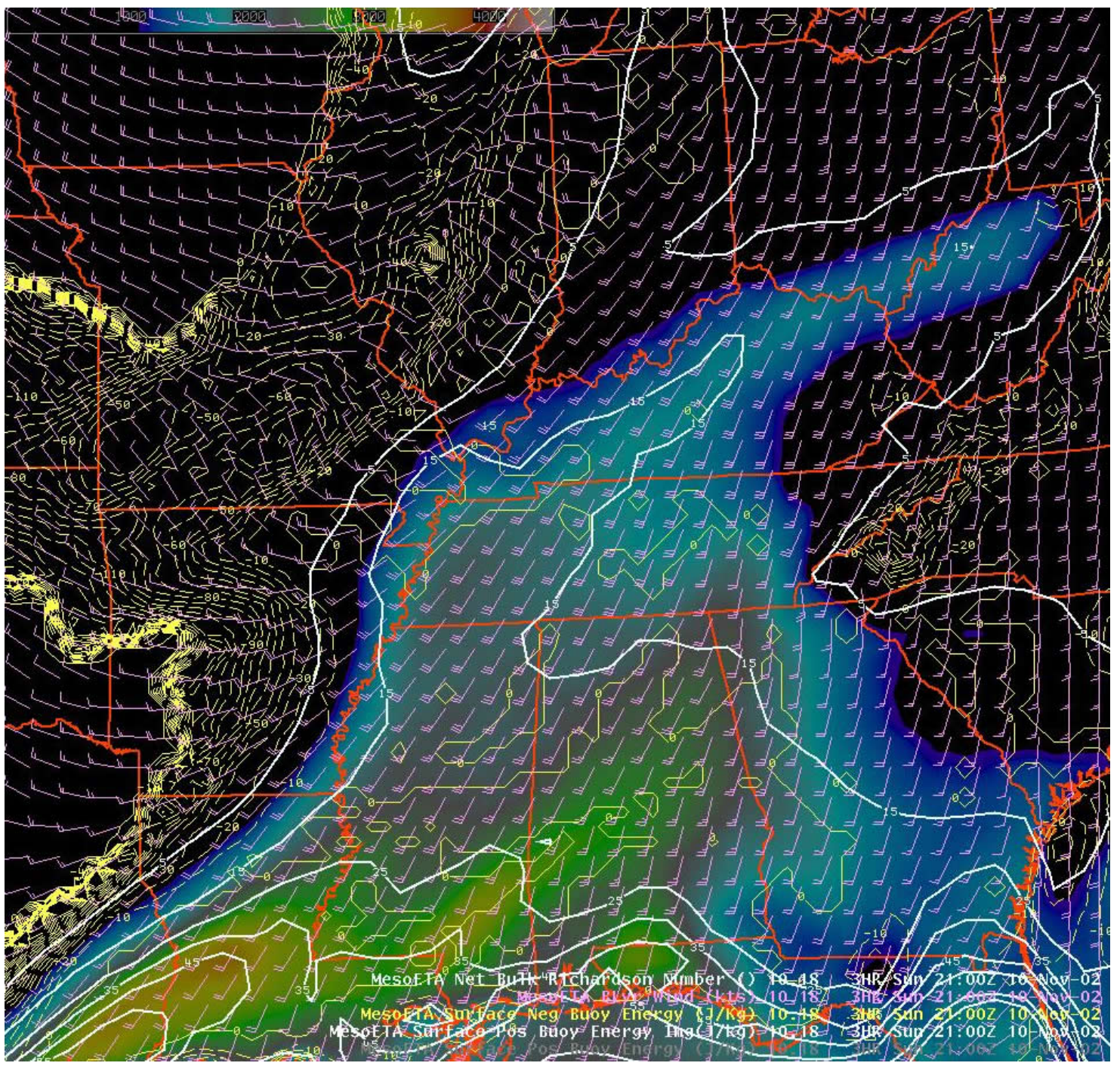


Figure 11

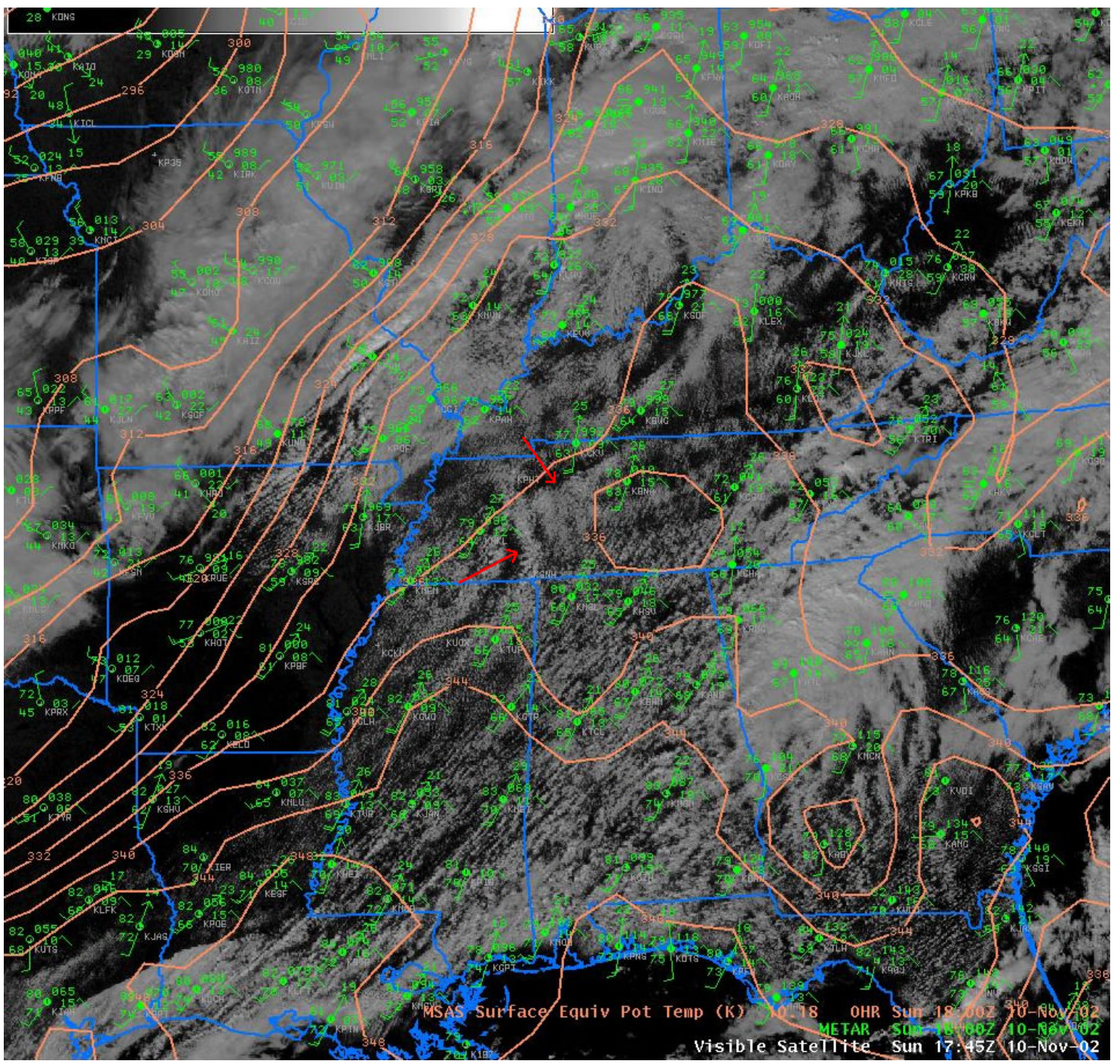


Figure 12

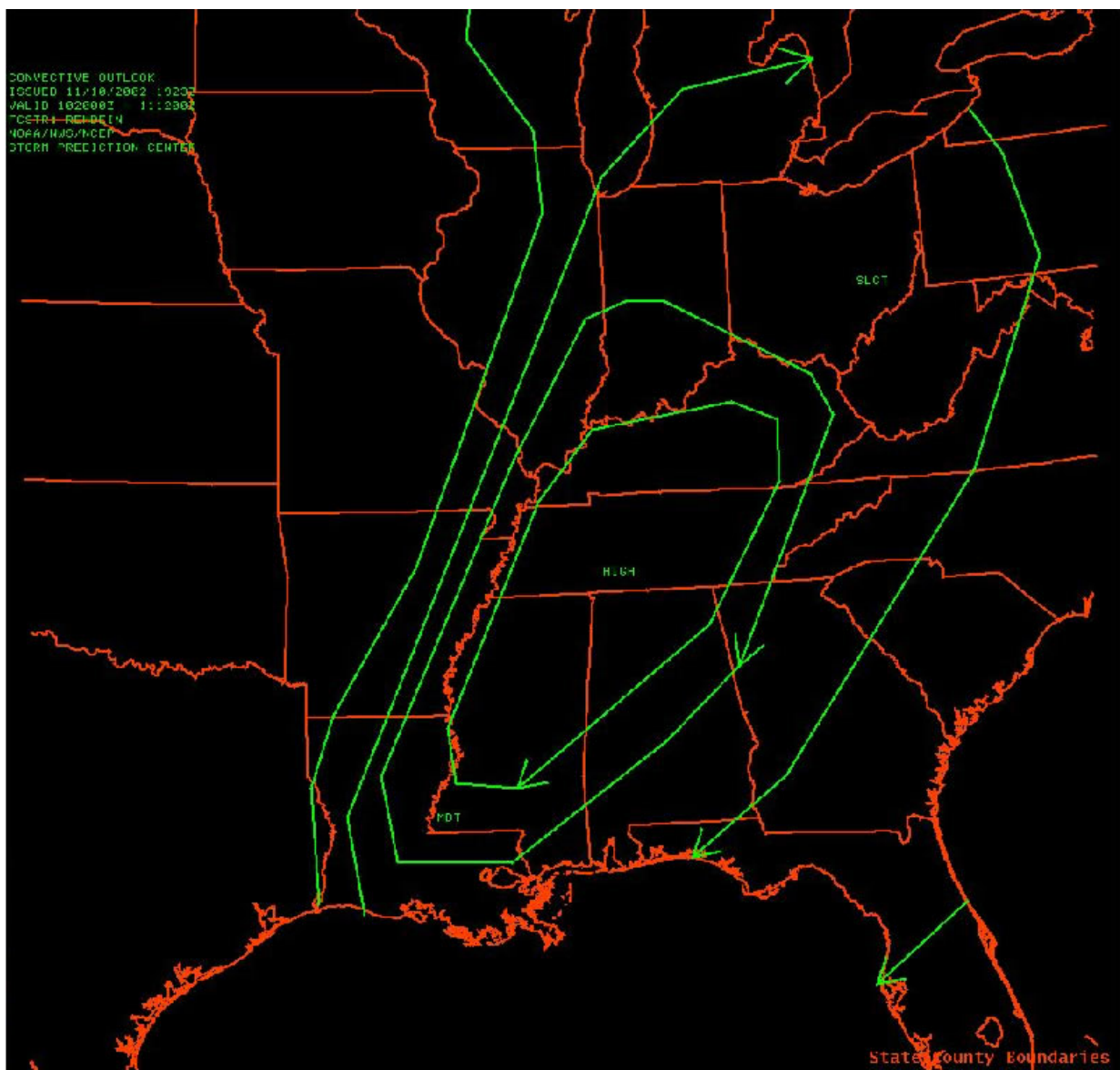


Figure 13

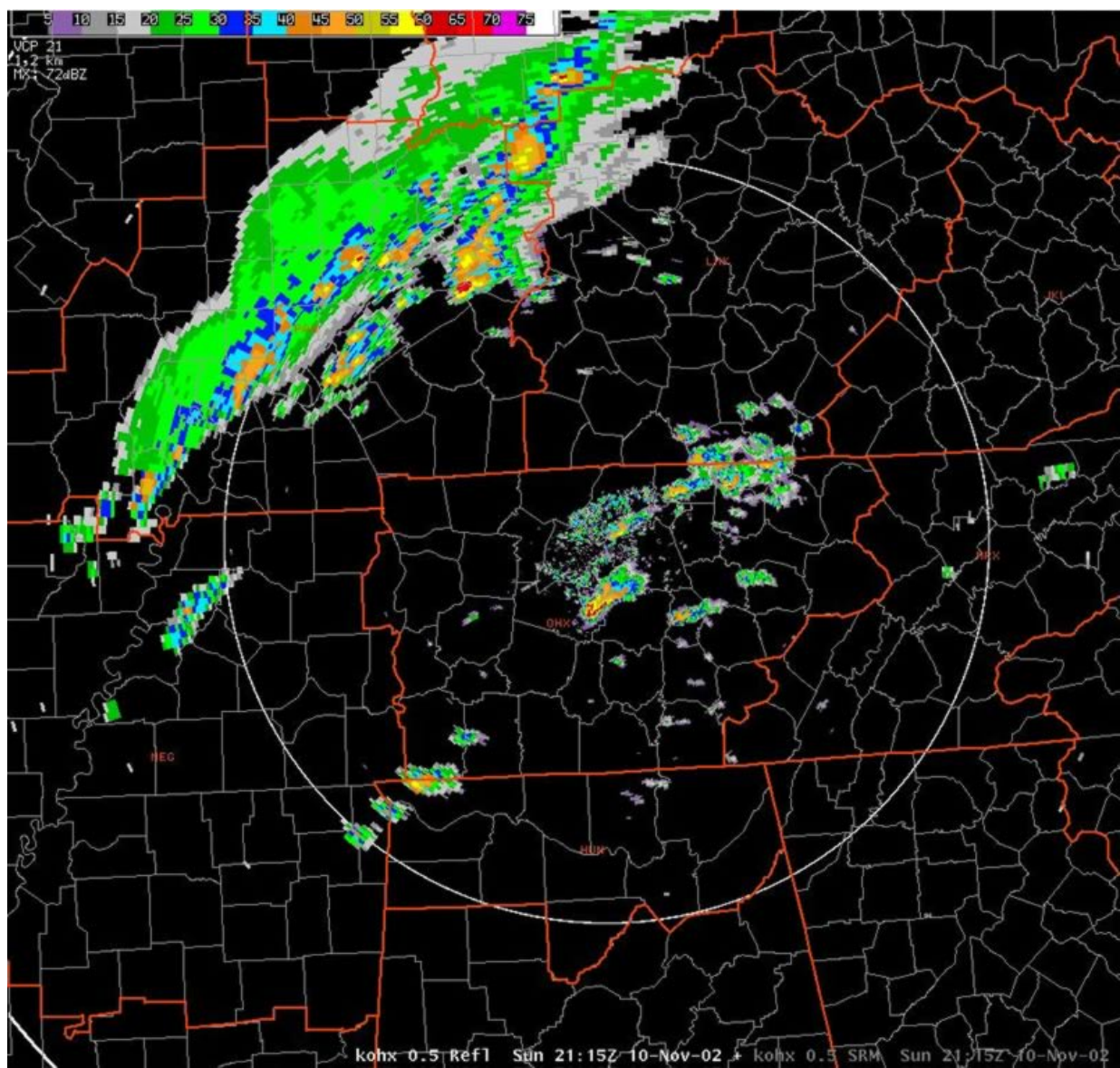


Figure 12

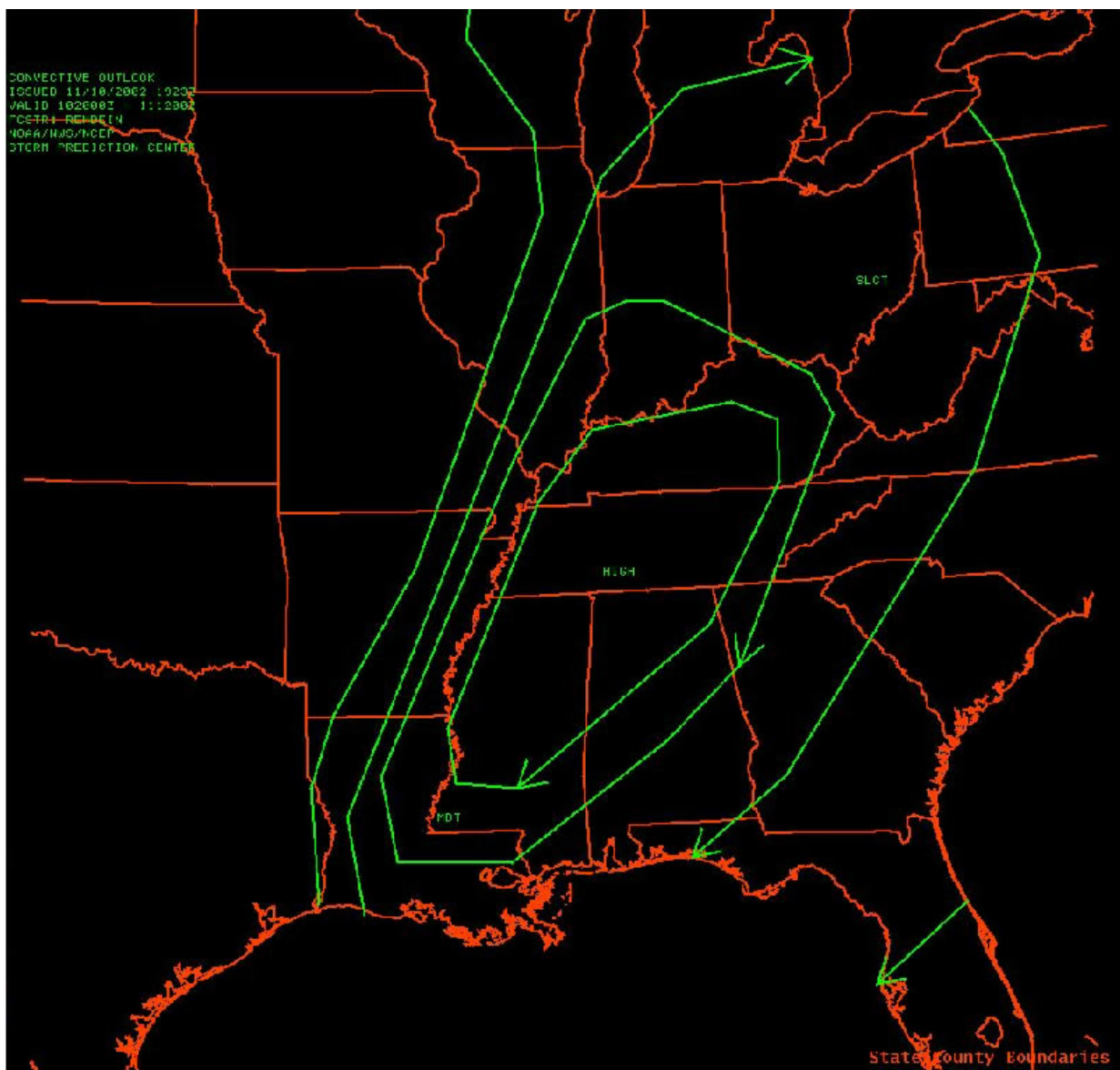


Figure 13

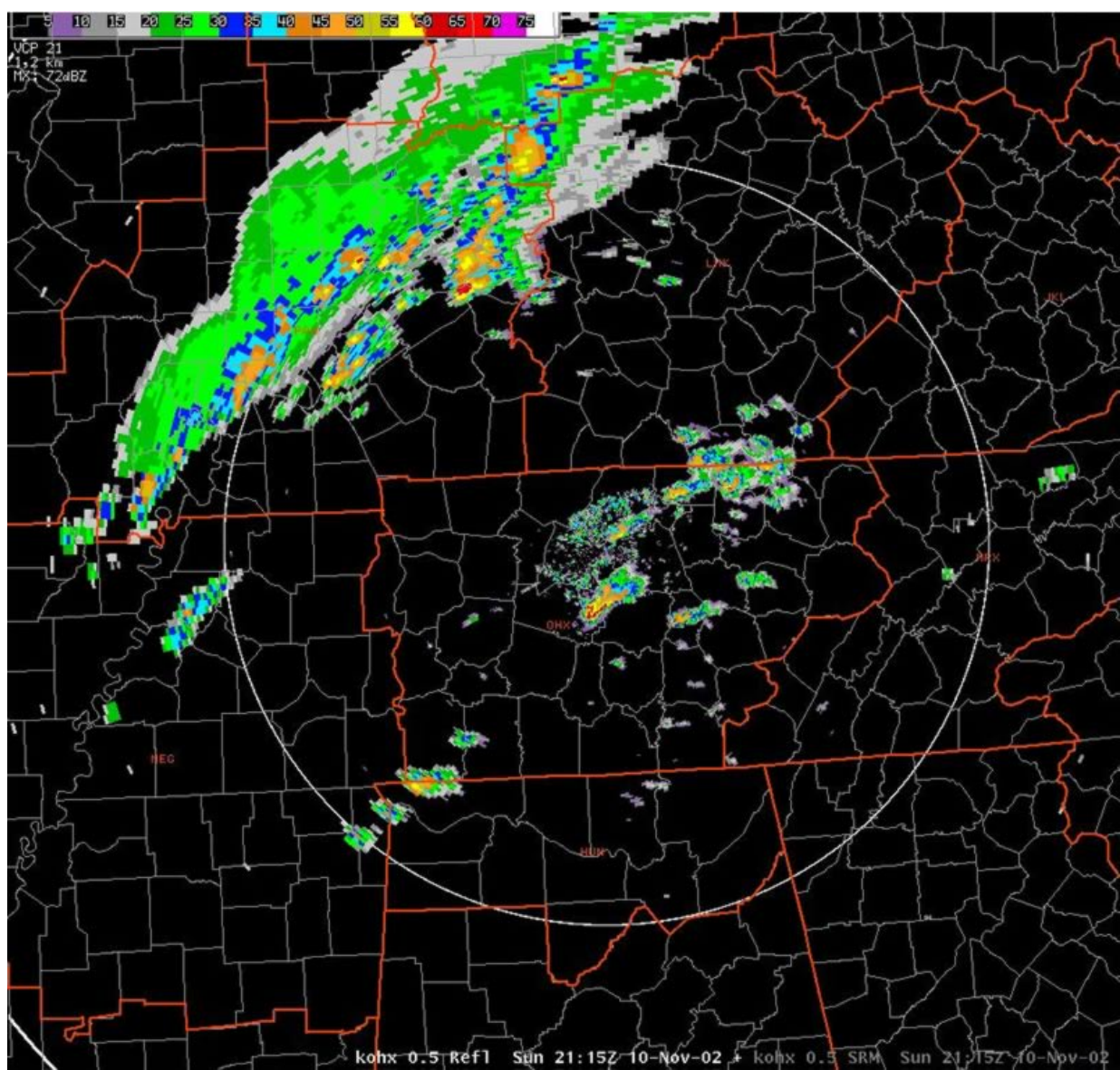


Figure 14



Figure 15

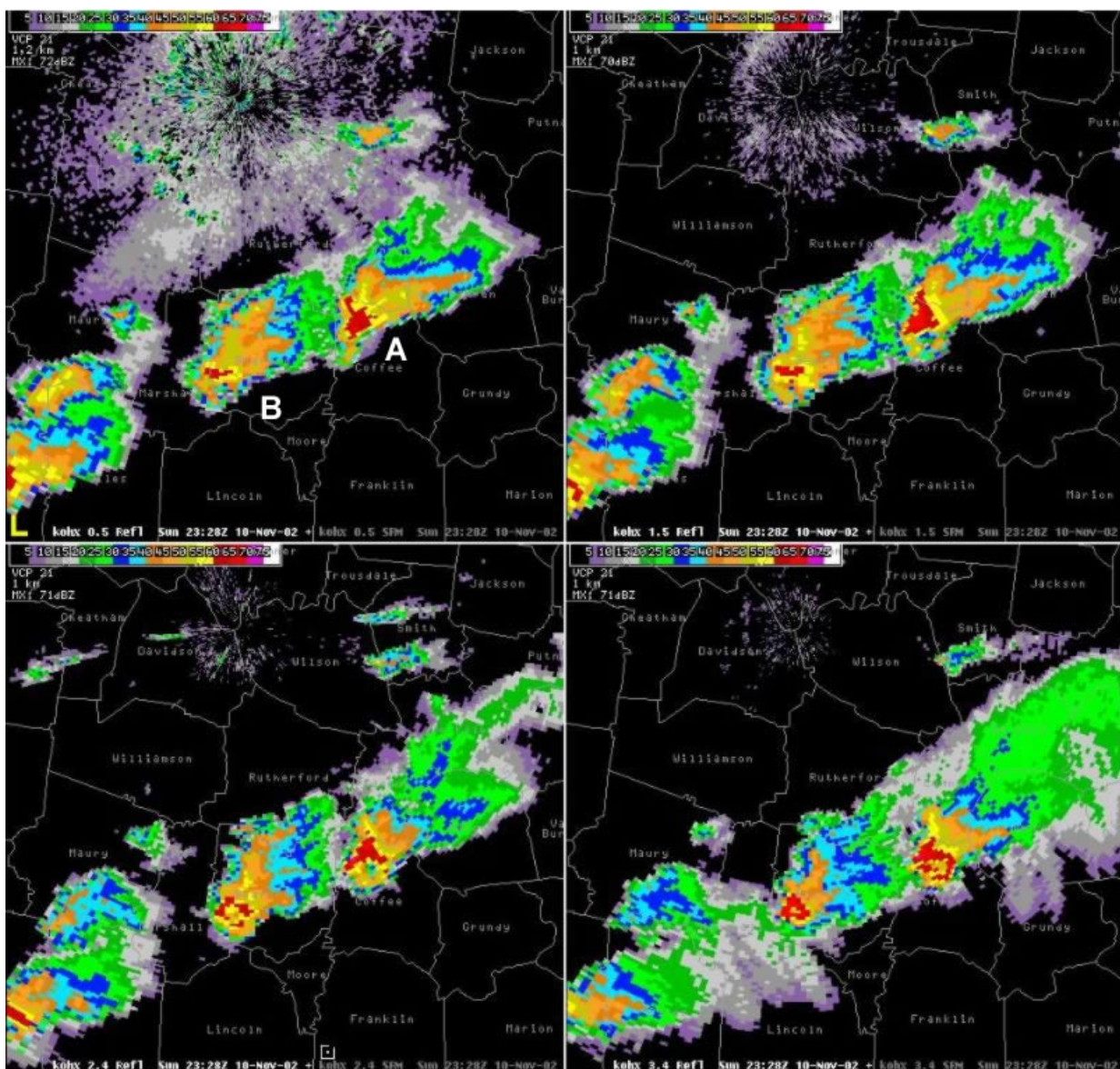


Figure 16

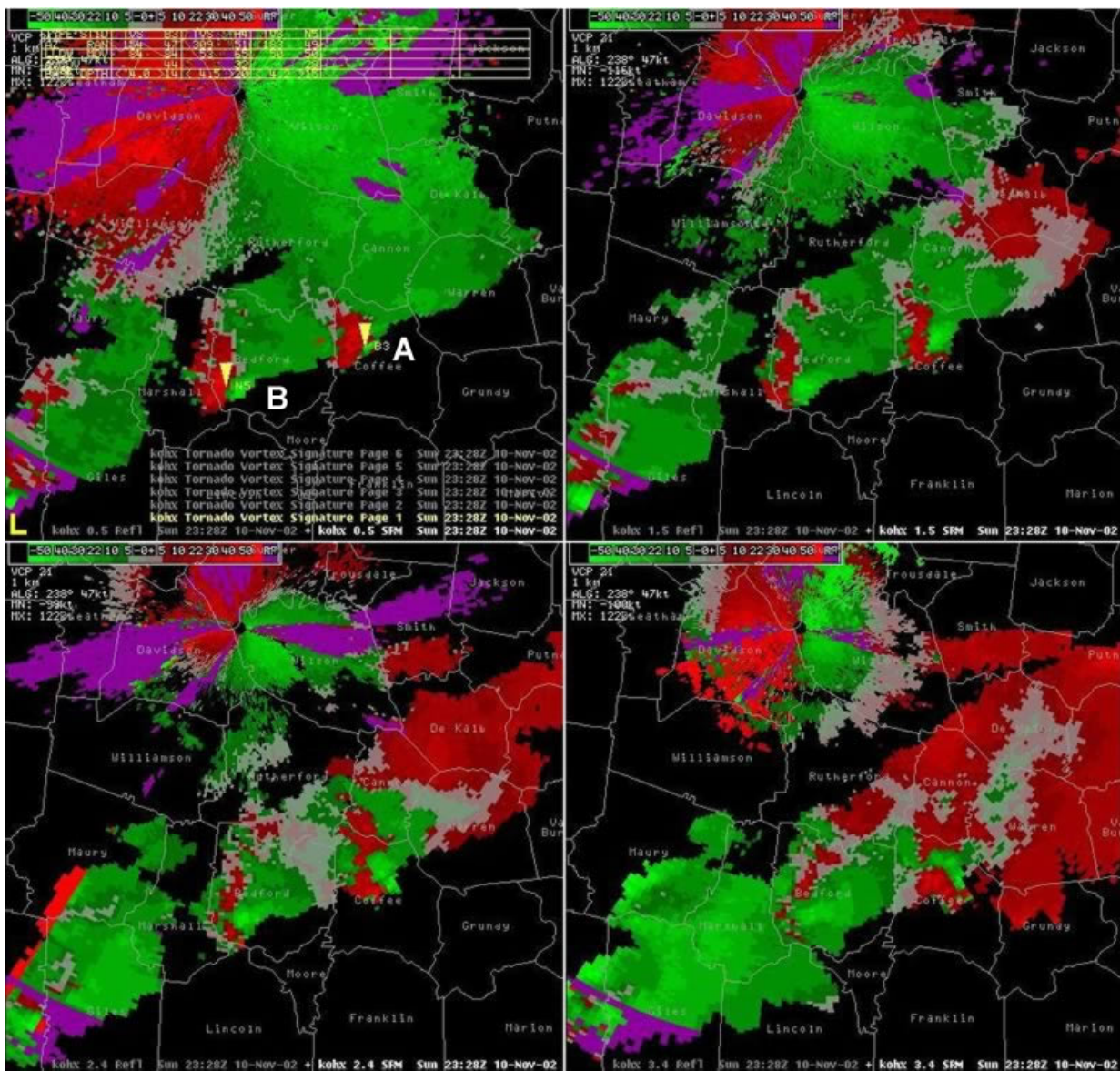


Figure 17

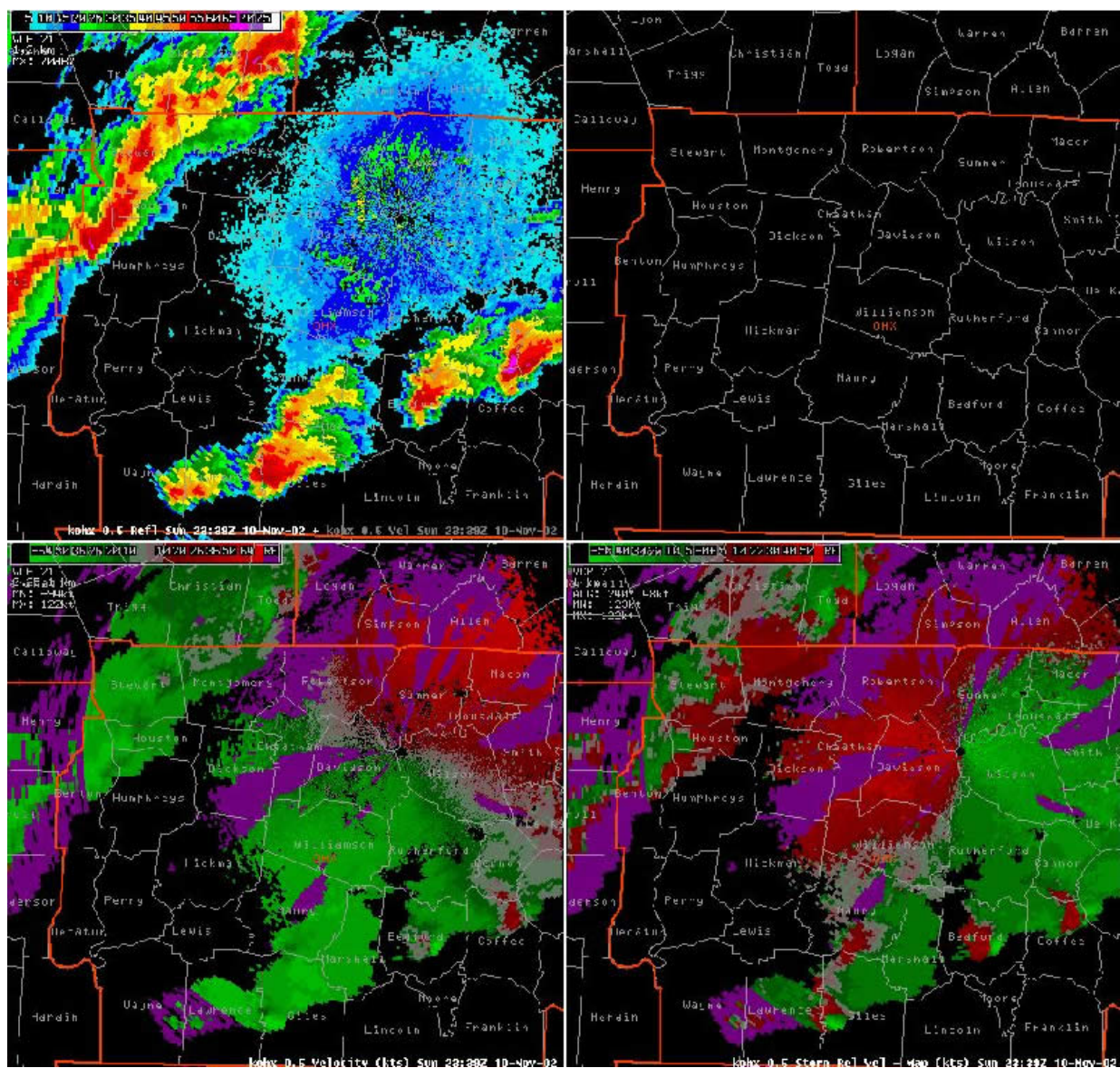


Figure 18

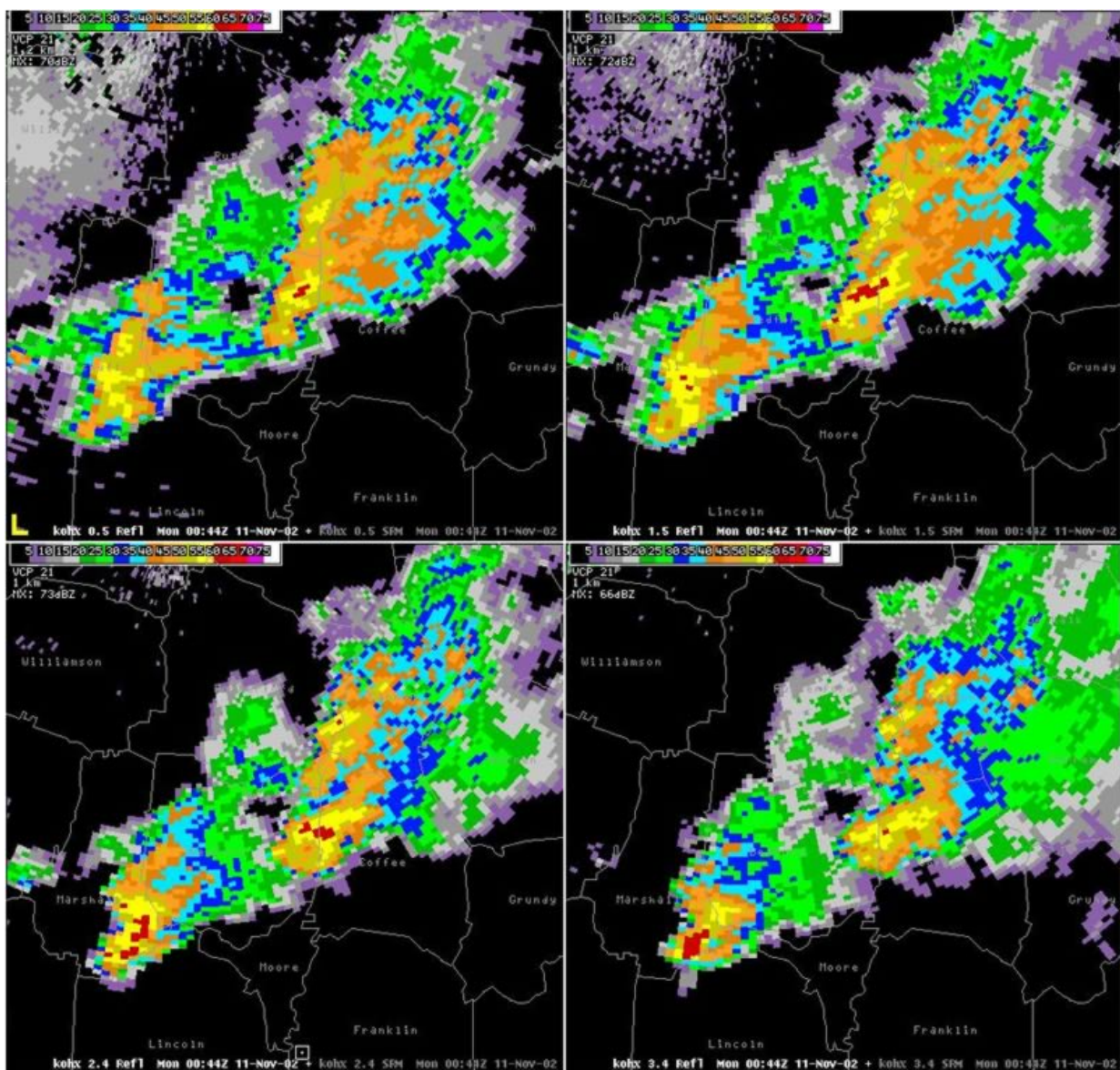


Figure 19

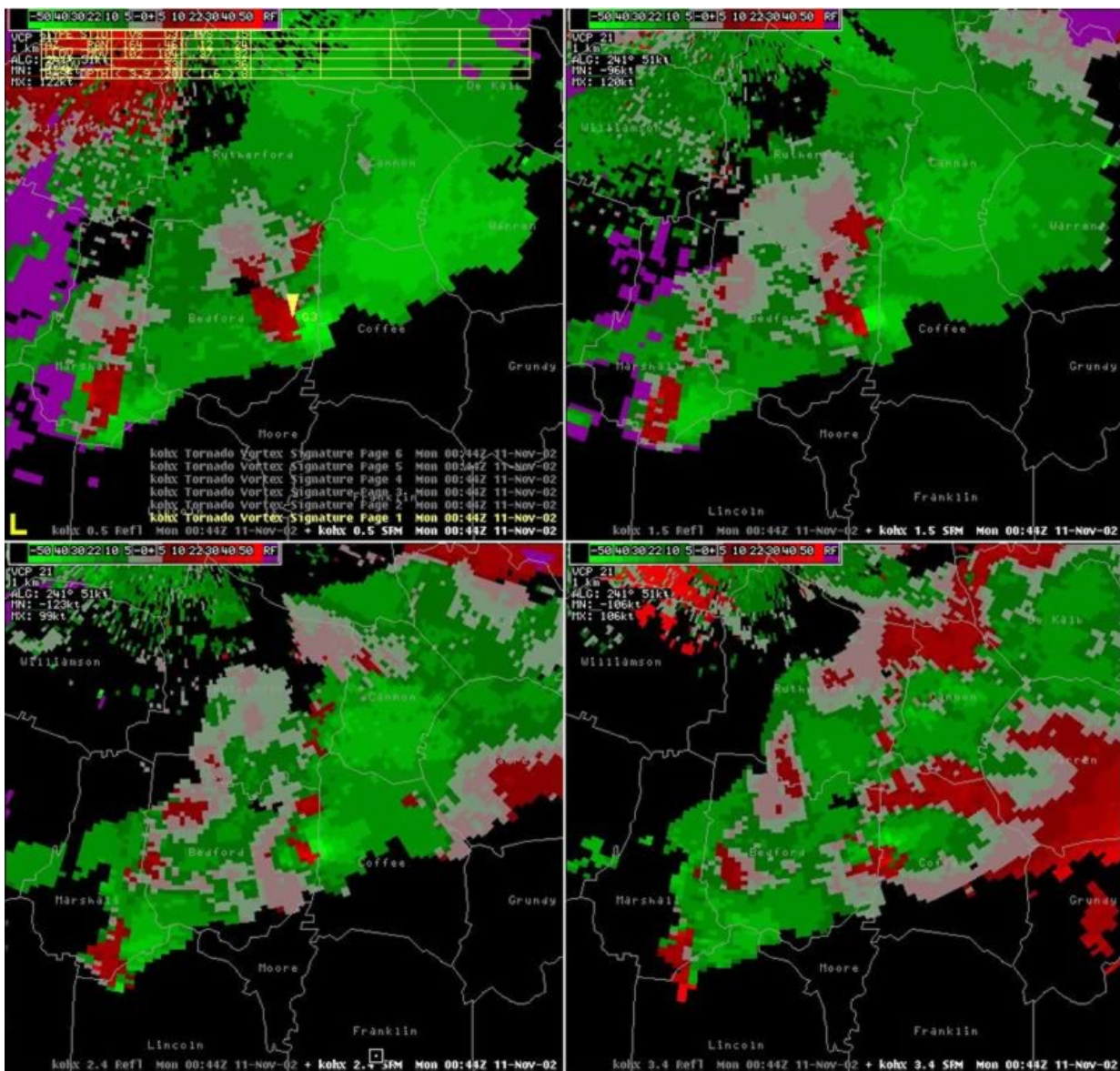


Figure 20

